CHEMISTRY
AN ASIAN JOURNAL
www.chemasianj.org

Accepted Article

Title: Steric twist effect-induced different ternary memory characteristics in non-conjugated copolymers with pendant naphthalene and 1,8-naphthalimide moieties

Authors: Ming Wang, Zhuang Li, Hua Li, Jinghui He, Najun Li, Qingfeng Xu, and Jian-Mei Lu

To be cited as: *Chem. Asian J.* 10.1002/asia.201701044

Link to VoR: http://dx.doi.org/10.1002/asia.201701044

A Journal of
ACES Asian Chemical Editorial Society

A sister journal of Angewandte Chemie and Chemistry – A European Journal

WILEY-VCH

10.1002/asia.201701044

WILEY-VCH

Steric twist effect-induced different ternary memory characteristics in non-conjugated copolymers with pendant naphthalene and 1,8-naphthalimide moieties

Ming Wang,[a] Zhuang Li,[a] Hua Li, *[a] Jinghui He,[a] Najun Li,[a] Qingfeng Xu,[a] and Jianmei Lu*[a]

Abstract: In this paper, novel random copolymer **PMNN** and **PMNB** were designed and synthesized, and the memory devices Al/**PMNN** or **PMNB**/ITO both exhibit the ternary memory performance. The switching voltages of OFF-ON1 and ON1-ON2transitions for both memory devices are around -2.0 V and -3.5 V, respectively, and the ON1/OFF, ON2/ON1 current ratio are both up to 10^3. The observed tristable electrical conductivity switching could be attributed to field-induced conformational ordering of naphthalene ring in the side chain, and subsequent charge trapping of 1,8-naphthalimide moieties. More interestingly, through adjusting the connection sites of 1,8-naphthalimide moieties to tune the steric twist effect, different memory properties (**PMNN** with nonvolatile WORM memory behavior, while PMNB with volatile SRAM memory behavior) were achieved. This result will offer a guideline for the design of different high-performance multilevel memory devices via tuning steric effects of the chemical moieties.

Introduction

With the rapid growth of information industry, polymeric binary memory materials have attracted increasing attentions and have potential as replacements for traditional silicon-based semiconductors in the future due to the advantages of good solution processability, ease of miniaturization and tailored properties through molecular design.[1] Time till now, several switching mechanisms such as charge transfer (CT) effect, conductive filament formation, conformational change, and trapping/detrapping mechanism have been illustrated.[1e, 1h, 2] To meet the demand of high-density data storage (HDDS), one of the strategies considered is to realize multilevel (eg. ternary) memory devices, which can increase the data storage capacity exponentially from 2^n to 3^n.[3] Recently, Kang et al.[4] have reported a polymer-based ternary memory device through two mechanisms. However, the ternary memory performance is limited to nonvolatile memory, which is difficult to face the practical demand for various ternary memory types.[5] Thus, obtaining diversiform ternary polymeric memory devices are highly desirable.

Among all the conformation-induced electrical bistability systems, the polymers containing naphthalene (**PMN**) have obvious advantages, such as larger conjugated plane, excellent charge liquidity and high ON/OFF current ratio.[6] Being structurally similar to naphthalene group, 1,8-naphthalimide moiety is a well-known electron-withdrawing group which can serve as the charge traps to block the movement of the charge carriers.[7] Furthermore, it is possible to utilize the different steric effects of 1,8-naphthalimide moieties through different connection sites to tune the memory behaviors.[7a, 7c, 8] Therefore, we hope to introduce 1,8-naphthalimidemoieties in PMN to achieve different ternary polymer memory devices.

Herein, we designed and synthesized two pendant copolymers, **PMNB** and **PMNN**, with different connection sites of 1,8-naphthalimide moieties, as shown in **Figure 1a**. The various connection sites of 1,8-naphthalimide exhibited different steric effects in polymer chains (**Figure S1**). Consequently, the Al/polymer/ITO devices exhibit different ternary memory behaviors. **PMNB** device shows volatile SRAM memory behavior, while **PMNN** exhibits nonvolatile WORM memory behavior. This result may offer a guideline for the design for various high-performance multilevel memory performances via tuning steric effects of the chemical moieties.

Results and Discussion

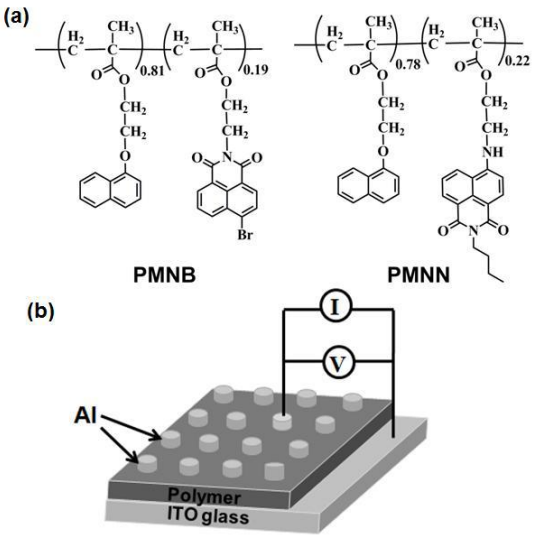

Figure 1. (a) Molecular structures of **PMNB** and **PMNN**; (b) A schematic diagram of the ITO/polymer/Aldevice.

PMNN and **PMNB** were synthesized in cyclohexanone solution by free radical copolymerization [**Scheme 1; see the Supporting Information (SI)**]. The chemical structures of

[a] M. Wang, ZH.Li, Prof. H. Li, Prof. J. He, Prof. N. Li,Prof. Q. Xu, Prof. J. Lu
College of Chemistry, Chemical Engineering and Materials Science, Collaborative Innovation Center of Suzhou Nano Science and Technology
Soochow University
Suzhou 215123, P. R. China
E-mail: jinghhe@suda.edu.cn, lujm@suda.edu.cn

Supporting information for this article is given via a link at the end of the document.

random copolymers and the relative ratios of electron donor/acceptor segments were confirmed by the ^{1}H NMR spectra (**Figure S2 and S3, SI**). The relatively molecular weights (Mw) of **PMNB** and **PMNN**, obtained by GPC using THF as the eluent and methyl methacrylate as standards, were 11300 and 17500g·mol^{-1} with the polydispersity index (PDI) of 1.48 and 1.97separately.Both random copolymers exhibited good thermalstability with an onset decomposition temperature of about 300 ^{o}C The Tg data of PMNB and PMNN are 106^{o}C and 110^{o}C calculated by DSC. (**Figure S4, SI**), implying that both copolymers are capable to endure heat deterioration in memory devices.[9]

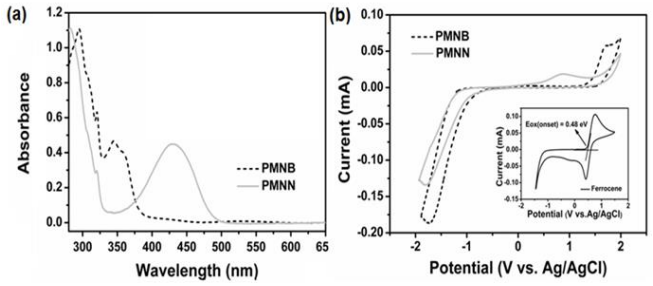

Figure 2. (a) UV-vis absorption spectra of the **PMNB** and **PMNN** films on quartz plate. (b) Cyclic voltammogram of **PMNB** and **PMNN** thin films spin-coated on ITO substrates in CH3CN containing 0.1 M TBAP at a scan rate of100 mV·s-1. The inset shows the CV curve of the ferrocene standard swept in the same conditions as for the two polymers ($E^{1/2}$ (ferrocene) was measured to be 0.48 eV vs. Ag/AgCl in CH_3CN).

UV-vis absorption spectra and cyclic voltammogram of **PMNB** and **PMNN** films were measured to study photophysical and electron chemical properties, respectively (Figure 2).The characteristics data of **PMNB** and **PMNN** are summarized in Table 1.The highest occupied molecular orbital (HOMO) and lowest unoccupied molecular orbital (LUMO) of **PMNB** and **PMNN** are calculated to be –5.05 eV/-2.32 eV and -5.07eV/-2.97 eV, respectively. Therefore, hole injection energy barriers of ITO/HOMO are smaller than the electron injection energy barriers of Al/LUMO, indicating that the conduction processes are dominated by hole injection.[10] Atomic force microscopy (AFM) images show that both films are quite smooth with root-mean-square (RMS) roughness of about 1.5 nm (Figure S5, SI). The observed smooth morphology of thin films is beneficial for the charge injection from the electrode into the polymer films.[11]

Table 1. optical and electrochemical properties of basic units and random copolymers in the DMF solution.

	E_{ox} (eV)	E_{red} (eV)	HOMO (eV)	LUMO (eV)	Φ_{ITO}-HOMO (eV)	LUMO-Φ_{Al} (eV)
PMNB	0.88	-0.09	-5.05	-2.32	0.25	1.98
PMNN	0.91	-0.11	-5.07	-2.97	0.27	1.33

Figure 1b is the schematic diagram of the ITO/polymer/Al memory device, which contains a about 80 nm thick film that sandwiched between an ITO bottom electrode and an aluminum top electrode (**Figure S6**). The typical *I-V* characteristics of memory devices in steps of 0.1 V are shown in **Figure 3**. For the case of **PMNN** (**Figure 3a**), the device initially starts with low-conductivity state (OFF state) and the current increased slowly until the turn-ON voltage. When a negative voltage is about –2.0 V, an abrupt increase in the current take place from 10^{-9} to 10^{-6} A, indicating that the device undergoes a sharp electrical transition from a low conductivity state(OFF state) to an intermediate conductance state (ON1 state). As the voltage approaches –3.2 V, a second sharp leap in current is observed from 10^{-5} to 10^{-2} A, indicating the transition from an intermediate conductance state (ON1 state) to a high conductance state (ON2 state)(sweep 1). The PMNN memory device exhibits the distinctly tristable conductance state with ON1/OFF, ON2/ON1 current ratio both up to 10^3, and these OFF-ON1 and ON1-ON2transitions that response to an external voltage can serve as a "writing" process in the memory cell. After a subsequent scan from 0 to –6.0 V, the memory device can be remained in ON2 state even after removing the power supply (sweep 2). This memory device, therefore, demonstrates typical non-volatile WORM-type memory behavior.[12]

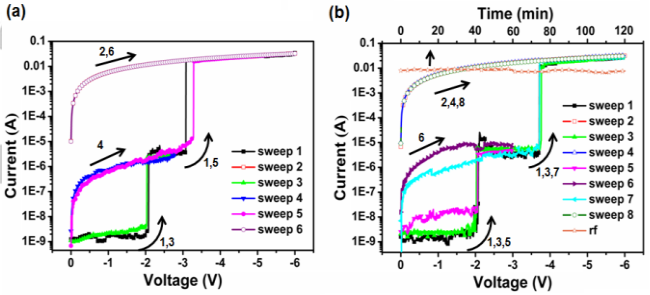

Figure 3. Typical *I-V* characteristics of the ITO/**PMNN**/Al (a) and the ITO/**PMNB**/Al (b) in the OFF, ON1 and ON2 state.

The electrical switching characterization of **PMNB** is shown in **Figure 3b**, which is different from that fabricated with **PMNN**. Similarly, the device is also initially at the OFF state. When a negative voltage is applied, two abrupt increases in the current can be observed around –1.96 V and –3.70 V, respectively. However, the device can be reprogrammed from the OFF to ON1 or ON2 state after removing the power about 5 min (sweep 3), indicating the device is rewritable. Besides, the voltage sweeping from 0 to –3.0 V (sweep 5, 6) and 0 to –6.0 V (sweep7 8) was successively performed. Thus, it can be concluded that **PMNB** based memory device exhibits the volatile nature of a static random access memory (SRAM).[13] The unstable ON2 state of the volatile memory device can be retained by a refreshing voltage pulse (named as the rf trace) of –1.0 V within 1 ms duration every 5 s.

The long-term stability and endurance performance are also evaluated from the retention time and stimulus effect test under the same atmosphere (**Figure S7, SI**). Figure S6 shows that the **PMNB** and **PMNN** devices could endure over 10^8 continuous read pluses of –1.0 V and no significant degradation in the current for any state is observed for 100 min. It is noteworthy that the writing voltages are all smaller than –4.0 V and the

reading voltage is as low as –1.0 V, which imply low power consumption of the **PMNB** and **PMNN** device during practical data-storage process.

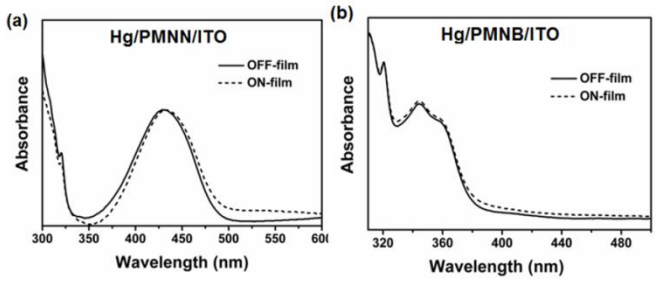

Figure 4. the ex-situ UV-vis spectra of the **PMNN** (a) and **PMNB (b)** thin films in the low-conductivity (OFF state) and high-conductivity (ON1 state). The **ON1** state was induced using a removable liquid-Hg droplet as the top electrode.

Huang and Ree al. once reported the conformational change of a single polymer to realize binary memory behavior through making disoriented pendant groups form oriented face-to-face conformation under an electrical field.[14] X-ray diffraction (XRD) analysis was first measured to ensure the low degree of regioregularity in copolymer **PMNN** or **PMNB** film at the ground state (**Figure S8**). When a negative bias (0 to –2.5 V) was applied, the holes injected from electrode (ITO) to the naphthalene groups near the interface (because the content of naphthalene groups is significantly higher than that of 1,8-naphthalimide) to form active species. Subsequently, attracted by the active naphthalene species, the neighboring neutral naphthalene or 1,8-naphthalimide groups tended to form a partial or full face-to-face conformation, through which the holes are delocalized to the neighboring naphthalene groups to form a conducting channel.

The UV-vis and PL spectra measurements of **PMNB** or **PMNN** thin film before and after the sweeping voltage from 0 to –2.5 V were analyzed to verify conformational change mechanism,[14b, 15] as shown in **Figure 4**. After the voltage sweep, UV-vis showed a red shift (for **PMNN** film) because of the ordered π-π stacking of naphthalene aromatic ring.[16] While **PMNB** film only exhibits slight broadening, indicating lower degree of regioregularity compared to polymer **PMNN**.[10b, 14a] High sensitivity fluorescence spectrum (**Figure S9**) further confirmed the conformational change phenomena of these two polymers.[17]

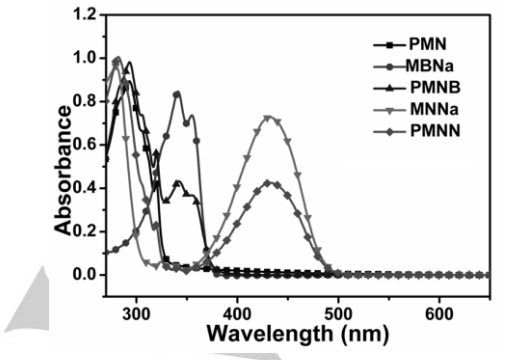

Figure 5. UV-vis absorption spectra of the PMN, MBNa, MNNa, PMNB and PMNN in DMF.

The optical properties of basic units and **PMNB** or **PMNN** (**Figure 5**) were measured to better understand the charge trapping switching progress. The main absorption peaks of **PMNB** and **PMNN** are identified by a linear superposition of the absorption on **PMN**, **MBNa** and **MNa**.[18] Thus, the charge transfer (CT) between the naphthalene donor and 1,8-naphthalimide acceptor is relatively weak. Density functional theory (DFT) molecular simulation results showed an open channel with negative molecular electrostatic potential (ESP) regions in blue, which were attributed to the 1,8-naphthalimide groups (**Figure S10**). These negative regions can serve as ''charge traps'' to block the mobility of the charge carriers. Thus, the second switching behavior is originated from the 1,8-naphthalimide trapping instead of the CT effect. With the increase of the voltage scan, the generated holes with sufficient activation energy will inject into thin film layer to fill the 1,8-naphthalimide traps. Consequently, the charge traps will full of charges, thus forming another conducting channel to result in high-conductivity state. [19]

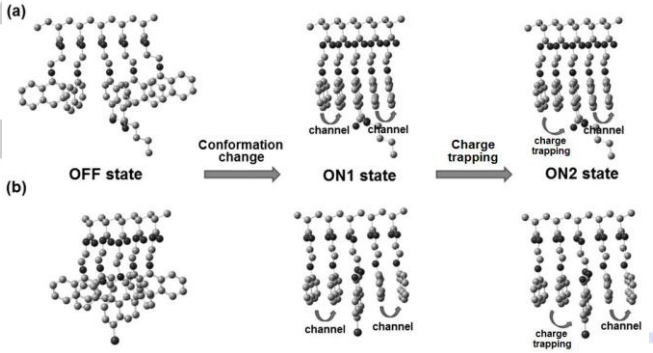

Figure 6. Schematic diagram of the charge carrier transport process in the polymer **PMNN** and **PMNB** based memory device.

To better understand the switching behavior of these devices, we diagramed the operational mechanism models,[1e] as depicted in **Figure 6**. The ternary memory device fabricated with **PMNN** or **PMNB** can be assigned to the conformation-induced conductance switching of naphthalene rings (OFF to ON1 state) and the subsequent charge trapping of 1,8-naphthalimide (ON1 to ON2 state). For **PMNN**, the flexible chain was connected to 1,8-naphthalimide group of the 4-site, after applying the voltage, the region-random of naphthalene groups transitioned to a region-regular ordering, and due to the similar arrangement of naphthalene groups and 1,8-naphthalimide, the formed ordered conformation was stable, thus it is difficult to return to the original OFF state even shutting down the applied voltage. While for **PMNB**, the flexible chain was connected to 1,8-naphthalimide group of the N-site, which will cause the steric hindrance of 1,8-naphthalimide groups in **PMNB**, thus leading to conformational relaxation from the region-regular arrangement to a region-random states of the pendant 1,8-naphthalimide moieties.

Conclusions

In conclusion, two new random copolymers **PMNN** and **PMNB** containing a flexible spacer and electron-accepting 1,8-naphthalimide were designed and synthesized. They both have high quality thin films but display different ternary memory behaviors. According to the analysis, the memory behaviors were achieved by combining dual mechanisms, conformational change and charge trapping mechanism. The different memory behaviors of **PMNN** and **PMNB** were caused by different connection sites of 1,8-naphthalimide moieties thus leading to different steric twist effects in polymers. This work offers fundamental insight for the rational design of ternary memory materials for polymer memory devices.

Experimental Section

Device Fabrication and Characterization: The indium tin oxide (ITO) glass was precleaned sequentially with deionized water, acetone and ethanol in ultrasonic bath each for 20 min, respectively. The copolymer was dissolved in cyclohexanone (12 mg·mL^{-1}) and filtered through micro filters with a pinhole size of 0.22 mm, Thereafter, the solutions were spin-coated onto ITO at 2000 rpm and the solvent was removedin a vacuum chamber at 10^{-1} Pa and 50 ^{o}C for 12 h. The thickness of the polymer layer was about 80 nm. Finally, the top Al electrode of 100 nm thick was thermally evaporated through a shadow mask under a pressure of 5×10^{-6}torr. The active area of each cell was 0.126 mm^2 (anummular point with a radius of 0.2 mm). All electrical measurements of the device were characterized under ambient conditions, using a HP 4145B semiconductor parameter analyzer.

^{1}H NMR spectra were obtained on an Inova 400MHz FT-NMR spectrometer. UV-vis absorption spectra were recorded by a PerkinElmer Lambda-17 spectrophotometer at room temperature. Thermogravimetric analysis (TGA) was conducted on a TA instrument Dynamic TGA 2950 at a heating rate of 20 ^{o}C·min^{-1} under a nitrogen flow rate of 100 mL·min^{-1}. Cyclic voltammetry was performed at room temperature using an ITO working electrode, a reference electrode of Ag/AgCl, and a counter electrode (Pt wire) at a scanning rate of 100 mV·s^{-1} (CorrTest CS Electrochemical Workstation analyzer) in a solution of tetrabutylammonium perchlorate (TBAP) in acetonitrile (0.1 M). SEM images were taken on a Hitachi S-4700 scanning electron microscope. Molecular weights (Mw) and polydispersity (Mw/Mn) was measured by gel permeation chromatography (GPC) utilizing a Waters 1515 pump and adifferential refractometer, THF was used as a mobile phase at a flow rate of 1.0 mL·min^{-1}.Differential scanning calorimetry (DSC) analyses were performed on a Shimadzu DSC-60A Instrument. Atomic force microscopy (AFM) measurements were performed by using a MFP-3DTM (Digital Instruments/Asylum Research) AFM instrument in tapping mode.

Acknowledgements

The authors gratefully thank the NSF of China (21336005 and 21476152), and National Excellent Doctoral Dissertation funds (201455).

Keywords:pendent copolymer • tristable switching • double mechanisms •steric effect

[1] a) S. J. Kim, J. S. Lee, *Nano Lett* **2010**, *10*, 2884-2890; b) Q.-D. Ling, D.-J. Liaw, E. Y.-H. Teo, C. Zhu, D. S.-H. Chan, E.-T. Kang, K.-G. Neoh, *Polymer,* **2007**, *48*, 5182-5201; c) S. J. Liu, P. Wang, Q. Zhao, H. Y. Yang, J. Wong, H. B. Sun, X. C. Dong, W. P. Lin, W. Huang, *Adv. Mater.* **2012**, *24*, 2901-2905; d) L. Sambe, V. R. de La Rosa, K. Belal, F. Stoffelbach, J. Lyskawa, F. Delattre, M. Bria, G. Cooke, R. Hoogenboom, P. Woisel, *Angew. Chem. Int. Ed.* **2014**, *53*, 5044-5048; e) L. H. Xie, Q. D. Ling, X. Y. Hou, W. Huang, *J. Am. Chem. Soc.* **2008**, *130*, 2120-2121; f) L.-H. Xie, C.-R. Yin, W.-Y. Lai, Q.-L. Fan, W. Huang, *Prog. in Polym. Sci.* **2012**, *37*, 1192-1264; g) A.-D. Yu, T. Kurosawa, Y.-C. Lai, T. Higashihara, M. Ueda, C.-L. Liu, W.-C. Chen, *J. Mater. Chem* **2012**, *22*, 20754; h) H. Zhuang, X. Xu, Y. Liu, Q. Zhou, X. Xu, H. Li, Q. Xu, N. Li, J. Lu, L. Wang, *J. Phys. Chem. C,* **2012**, *116*, 25546-25551.

[2] a) P. Y. Gu, F. Zhou, J. Gao, G. Li, C. Wang, Q. F. Xu, Q. Zhang, J. M. Lu, *J. Am. Chem. Soc.* **2013**, *135*, 14086-14089; b) C. S. Hwang, *Adv. Electron. Mater.* **2015**, *1*, 1400056.

[3] a) E. Y. Hong, C. T. Poon, V. W. Yam, *J. Am. Chem. Soc.* **2016**, *138*, 6368-6371; b) A. Kumar, M. Chhatwal, P. C. Mondal, V. Singh, A. K. Singh, D. A. Cristaldi, R. D. Gupta, A. Gulino, *Chem. Commun. (Camb)* **2014**, *50*, 3783-3785; c) C. T. Poon, D. Wu, W. H. Lam, V. W. Yam, *Angew. Chem. Int. Ed.* **2015**, *54*, 10569-10573.

[4] G. Liu, D. J. Liaw, W. Y. Lee, Q. D. Ling, C. X. Zhu, D. S. Chan, E. T. Kang, K. G. Neoh, *Philos. Trans. A Math. Phys. Eng. Sci.* **2009**, *367*, 4203-4214.

[5] a) M. J. Lee, Y. Park, D. S. Suh, E. H. Lee, S. Seo, D. C. Kim, R. Jung, B. S. Kang, S. E. Ahn, C. B. Lee, D. H. Seo, Y. K. Cha, I. K. Yoo, J. S. Kim, B. H. Park, *Adv. Mater.* **2007**, *19*, 3919-3923; b) J. C. Scott, L. D. Bozano, *Adv. Mater.* **2007**, *19*, 1452-1463.

[6] aY. Gao, G. P. Robertson, M. D. Guiver, S. D. Mikhailenko, X. Li, S. Kaliaguine, *Polymer,***2006**, *47*, 808-816; bG. Kim, S. J. Kang, G. K. Dutta, Y. K. Han, T. J. Shin, Y. Y. Noh, C. Yang, *J. Am. Chem. Soc.* **2014**, *136*, 9477-9483.

[7] a) S. M. Anderson, S. D. Mitchell, K. A. LaPlante, R. K. McKenney, D. E. Lewis, *J.Heterocycl. Chem.* **2017**, *54*, 2029-2037; b) T. T. Do, H. D. Pham, S. Manzhos, J. M. Bell, P. Sonar, *ACS Appl. Mater. Interfaces,* **2017**, *9*, 16967-16976; c) P. Gautam, R. Sharma, R. Misra, M. L. Keshtov, S. A. Kuklin, G. D. Sharma, *Chem. Sci.* **2017**, *8*, 2017-2024; d) H. Ulla, M. R. Kiran, B. Garudachari, T. N. Ahipa, K. Tarafder, A. V. Adhikari, G. Umesh, M. N. Satyanarayan, *J. of Mol. Struct.* **2017**, *1143*, 344-354; e) H.-H. Lin, Y.-C. Chan, J.-W. Chen, C.-C. Chang, *J. Mater. Chem.* **2011**, *21*, 3170.

[8] a) H.-J. Yen, J.-H. Chang, J.-H. Wu, G.-S. Liou, *Polym. Chem.* **2015**, *6*, 7758-7763; b) Y. Luo, Y. Wang, S. Chen, N. Wang, Y. Qi, X. Zhang, M. Yang, Y. Huang, M. Li, J. Yu, D. Luo, Z. Lu, *Small,* **2017**, *13*.

[9] a) R. Baruah, A. Kumar, R. R. Ujjwal, S. Kedia, A. Ranjan, U. Ojha, *Macromolecules,* **2016**, *49*, 7814-7824; b) F. Bella, G. Leftheriotis, G. Griffini, G. Syrrokostas, S. Turri, M. Grätzel, C. Gerbaldi, *Adv.Funct. Mater.* **2016**, *26*, 1127-1137; c) C. Ouyang, J. Liu, Q. Liu, Y. Li, D. Yan, Q. Wang, M. Guo, A. Cao, *ACS Appl. Mater. Interfaces,* **2017**, *9*, 10366-10370.

[10] a) D. Wi, J. Kim, H. Lee, N.-G. Kang, J. Lee, M.-J. Kim, J.-S. Lee, M. Ree, *J. Mater. Chem. C,* **2016**, *4*, 2017-2027; b) Y. Li, Z. Liu, H. Li, Q. Xu, J. He, J. Lu, *ACS App.l Mater. Interfaces,* **2017**, *9*, 9926-9934; cA. Corani, M. H. Li, P. S. Shen, P. Chen, T. F. Guo, A. El Nahhas, K. Zheng, A. Yartsev, V. Sundstrom, C. S. Ponseca, Jr., *J. Phys. Chem. Lett.* **2016**, *7*, 1096-1101.

[11] a) Z. Zhao, Z. Yin, H. Chen, Y. Guo, Q. Tang, Y. Liu, *J. Mater. Chem. C* **2017**, *5*, 2892-2898; b) Z. Zhao, Z. Yin, H. Chen, L. Zheng, C. Zhu, L. Zhang, S. Tan, H. Wang, Y. Guo, Q. Tang, Y. Liu, *Adv. Mater.* **2017**, *29*; c) K. Oniwa, H. Kikuchi, T. Kanagasekaran, H. Shimotani, S. Ikeda,

N. Asao, Y. Yamamoto, K. Tanigaki, T. Jin, *Chem. Commun. (Camb)* **2016**, *52*, 4926-4929.

[12] a) N. Jia, S. Qi, G. Tian, X. Wang, D. Wu, *J. Phys. Chem. C* ,**2016**, *120*, 26217-26224; b) C. C. Shih, C. Y. Chung, J. Y. Lam, H. C. Wu, Y. Morimitsu, H. Matsuno, K. Tanaka, W. C. Chen, *Chem. Commun. (Camb)* **2016**, *52*, 13463-13466.

[13] Y.-C. Lai, Y.-X. Wang, Y.-C. Huang, T.-Y. Lin, Y.-P. Hsieh, Y.-J. Yang, Y.-F. Chen, *Adv. Funct. Mater.* **2014**, *24*, 1430-1438.

[14] a) W. Kwon, B. Ahn, D. M. Kim, Y.-G. Ko, S. G. Hahm, Y. Kim, H. Kim, M. Ree, *J. Phys. Chem. C,* **2011**, *115*, 19355-19363; b) W. P. Lin, S. J. Liu, T. Gong, Q. Zhao, W. Huang, *Adv. Mater.* **2014**, *26*, 570-606.

[15] a) C. Mi, R. Tan, D. Sun, Z. Ren, X. Sun, S. Yan, *J. Mater. Chem. C,* **2015**, *3*, 10249-10255; b) S. T. Han, Y. Zhou, V. A. Roy, *Adv. Mater.* **2013**, *25*, 5425-5449; c) R. C. Shallcross, P. Zacharias, A. Köhnen, P. O. Körner, E. Maibach, K. Meerholz, *Adv. Mater.***2013**, *25*, 469-476.

[16] a) W. Wang, Y. Li, L. Cheng, Z. Cao, W. Liu, *J. Mater. Chem. B* **2014**, *2*, 46-48; b) D. Mondal, M. Bar, D. Maity, S. Baitalik, *J. Phys. Chem. C,* **2015**, *119*, 25429-25441.

[17] H.-J. Kim, J. Sung, H. Chung, Y. J. Choi, D. Y. Kim, D. Kim, *J.Phys.Chem. C,* **2015**, *119*, 11327-11336.

[18] W. Li, Y. Pan, R. Xiao, Q. Peng, S. Zhang, D. Ma, F. Li, F. Shen, Y. Wang, B. Yang, Y. Ma, *Adv. Funct. Mater.* **2014**, *24*, 1609-1614.

[19] a) S. Miao, H. Li, Q. Xu, Y. Li, S. Ji, N. Li, L. Wang, J. Zheng, J. Lu, *Adv. Mater.* **2012**, *24*, 6210-6215; b) Y. Li, H. Li, J. He, Q. Xu, N. Li, D. Chen, J. Lu, *Chem. Asian. J.* **2016**, *11*, 906-914; c) H. Liu, R. Bo, H. Liu, N. Li, Q. Xu, H. Li, J. Lu, L. Wang, *J. Mater. Chem. C,* **2014**, *2*, 5709-5716.

10.1002/asia.201701044

FULL PAPER

Due to the adjusting of the connection sites of 1,8-naphthalimide moieties to tune the steric twist effect, two novel random copolymer **PMNN** and **PMNB** exhibit different ternary memory performance through conformational change and charge trapping mechanism.

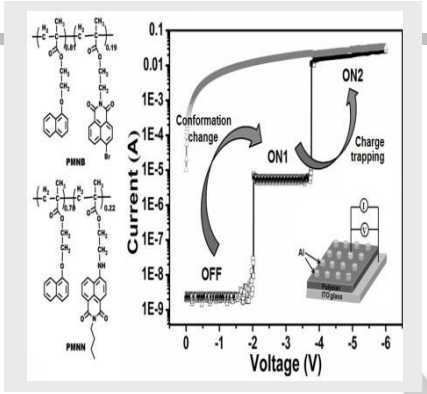

Ming Wang, Zhuang Li , Hua Li, Jinghui He, Najun Li, Qingfeng Xu and Jianmei Lu**

Page No. – Page No.

Steric twist effect-induced different ternary memory characteristics in non-conjugated copolymers with pendant naphthalene and 1,8-naphthalimide moieties